Electronic Supplementary Material (ESI) for RSC Advances.

Supporting Information

Structural imposition on *off-on* response of naphthalimide based probes for selective thiophenol sensing

Dnyaneshwar Kand,[a,‡] Prashant Sahebrao Mandal,[b,‡] Tanmoy Saha,[a] and Pinaki Talukdar*[a]

[a] *Department of Chemistry, Indian Institute of Science Education and Research Pune, India. Fax: +91 20 2589 9790; Tel: +91 20 2590 8001.*

[b] *Department of Chemistry, Institute of Chemical Technology (ICT), Mumbai 400019, India.*

‡ Equal contributions of both authors.

E-mail: ptalukdar@iiserpune.ac.in

Contents **Page Number**

I. Crystal Structures:

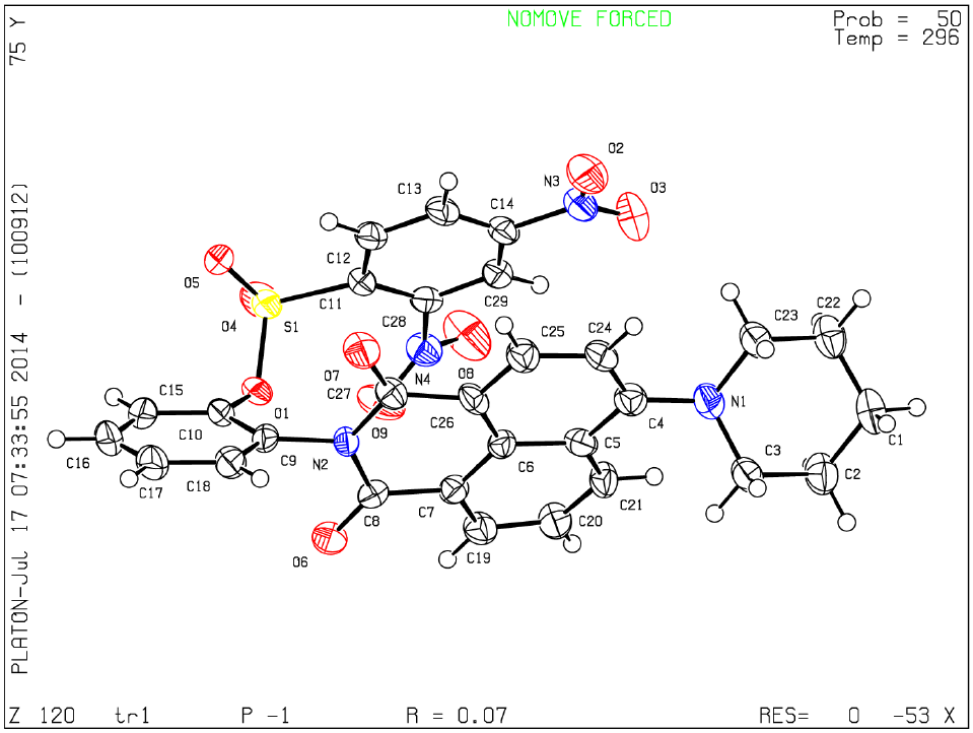

Fig. S1 ORTEP diagram of probe **4o**.

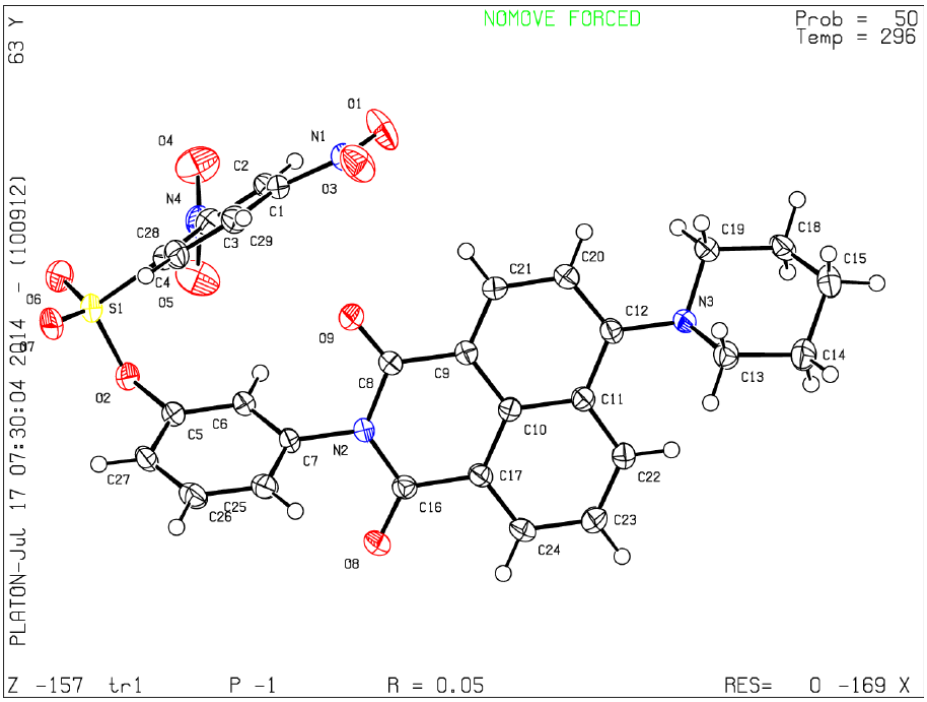

Fig. S2 ORTEP diagram of probe **4m**.

II. Theoretical Calculations:

The molecular geometries of **4o′**, **4m′** and **4p′** were fully optimized at a level of density functional theory employing the hybrid functional B3LYP with Pople's basis set 6-31G (d, p) where polarization functions were added to all the atoms and diffuse functions to the heavy atoms. All the calculations were performed with the development version of Gaussian 09.[S1]

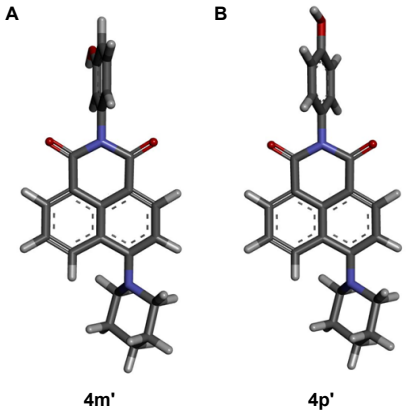

Fig. S3 Geometry optimized structure of **4m′**, and **4p′** by DFT B3LYP/6-31G (d,p) in gas phase.

Table S1. Atomic coordinates calculated for **4o′** from DFT B3LYP/6-31G (d, p) geometry optimization in gas phase.

Symbolic Z-matrix:

Charge = 0

Multiplicity = 1

Atom #	Atom Type	x	y	z
1	C	-0.0015	2.7601	0.1564
2	C	1.3857	2.9772	0.083
3	C	2.2564	1.9099	-0.0333
4	C	1.7814	0.5749	-0.0679
5	C	0.3694	0.3641	-0.0481
6	C	-0.5055	1.4717	0.0815
7	C	2.6551	-0.5669	-0.1856
8	C	2.0863	-1.8225	-0.3891
9	C	0.6949	-2.0043	-0.4
10	C	-0.1658	-0.9374	-0.2052
11	C	-1.6209	-1.1792	-0.1657
12	N	-2.4548	-0.0376	0.0635
13	C	-1.9704	1.2708	0.1117
14	O	-2.1081	-2.2875	-0.3021
15	O	-2.7474	2.229	0.1697
16	C	-3.877	-0.2791	0.2141

17	C	-4.2993	-1.1709	1.205
18	C	-5.6429	-1.5027	1.3388
19	C	-6.5817	-0.936	0.4726
20	C	-6.1763	-0.024	-0.4947
21	C	-4.8262	0.3234	-0.6332
22	N	4.0473	-0.3707	-0.1275
23	C	4.5907	0.052	1.1823
24	C	5.9893	0.6523	1.028
25	C	6.9307	-0.3316	0.321
26	C	6.3074	-0.818	-0.9934
27	C	4.8991	-1.3797	-0.7674
28	H	-0.6982	3.586	0.2466
29	H	1.7718	3.9914	0.0984
30	H	3.3207	2.086	-0.139
31	H	2.7238	-2.6917	-0.4972
32	H	0.2694	-2.9939	-0.5283
33	H	-3.5589	-1.6203	1.857
34	H	-5.9524	-2.2016	2.1089
35	H	-6.8872	0.4546	-1.1598
36	H	3.9071	0.7704	1.6367
37	H	4.6369	-0.8206	1.859
38	H	5.9192	1.581	0.4473
39	H	6.3767	0.9176	2.0184
40	H	7.906	0.1318	0.1362
41	H	7.1106	-1.194	0.9778
42	H	6.243	0.0143	-1.7048
43	H	6.9307	-1.5924	-1.4547
44	H	4.4452	-1.657	-1.7227
45	H	4.9678	-2.2973	-0.1537
46	H	-7.6333	-1.1921	0.5633
47	O	-4.4898	1.2233	-1.596
48	H	-3.8579	1.8441	-1.1785

Table S2. Atomic coordinates calculated for **4m′** from DFT B3LYP/6-31G (d, p) geometry optimization in gas phase.

Symbolic Z-matrix:

Charge = 0

Multiplicity = 1

Atom #	Atom Type	x	y	z
1	C	0.1265	2.7504	-0.5124
2	C	1.5186	2.9396	-0.5817
3	C	2.3778	1.8657	-0.4478
4	C	1.8852	0.554	-0.23
5	C	0.47	0.3584	-0.2257
6	C	-0.3929	1.4777	-0.3504
7	C	2.7491	-0.5895	-0.0682
8	C	2.1764	-1.8575	-0.0218
9	C	0.7835	-2.0341	-0.0554
10	C	-0.0712	-0.9493	-0.1302
11	C	-1.5321	-1.1739	-0.1222
12	N	-2.3442	-0.0183	-0.2127
13	C	-1.8679	1.3044	-0.3237
14	O	-2.0361	-2.2831	-0.0392
15	O	-2.6428	2.2456	-0.3937
16	C	-3.7779	-0.2107	-0.2038
17	C	-4.4891	0.051	0.9657
18	C	-5.8746	-0.1269	0.9819
19	C	-6.5384	-0.5733	-0.1657
20	C	-5.8092	-0.8331	-1.3224
21	C	-4.4255	-0.6521	-1.3543
22	N	4.1419	-0.386	0.0055
23	C	4.6309	0.2897	1.2272
24	C	6.0408	0.8456	1.0173
25	C	7.0029	-0.2607	0.5662
26	C	6.4317	-1.004	-0.6484
27	C	5.0091	-1.5058	-0.3749
28	H	-0.5635	3.5817	-0.6077
29	H	1.9181	3.9337	-0.756
30	H	3.4479	2.0099	-0.5433
31	H	2.8081	-2.7314	0.0846
32	H	0.3514	-3.0272	0.0081
33	H	-3.9631	0.3977	1.8508
34	H	-6.3257	-1.1801	-2.212

35	H	-3.8538	-0.8545	-2.2527
36	H	3.9354	1.0856	1.4967
37	H	4.6392	-0.4289	2.0673
38	H	6.004	1.6367	0.2574
39	H	6.388	1.3065	1.9491
40	H	7.989	0.156	0.3335
41	H	7.1484	-0.9719	1.3914
42	H	6.4052	-0.3326	-1.5153
43	H	7.0668	-1.8563	-0.9158
44	H	4.5944	-1.9734	-1.2722
45	H	5.0429	-2.2782	0.4163
46	H	-7.6142	-0.707	-0.1306
47	O	-6.632	0.117	2.0932
48	H	-6.0589	0.4343	2.8032

Table S3. Atomic coordinates calculated for **4p′** from DFT B3LYP/6-31G (d, p) geometry optimization in gas phase.

Symbolic Z-matrix:

Charge = 0

Multiplicity = 1

Atom #	Atom Type	x	y	z
1	C	0.219363	2.815134	-0.131736
2	C	1.611653	2.991527	-0.227281
3	C	2.456299	1.89807	-0.237797
4	C	1.948555	0.577622	-0.142985
5	C	0.53103	0.402363	-0.109563
6	C	-0.316472	1.539724	-0.087296
7	C	2.796525	-0.588815	-0.135623
8	C	2.202991	-1.84619	-0.203684
9	C	0.80681	-1.998464	-0.205124
10	C	-0.030309	-0.899938	-0.133422
11	C	-1.494048	-1.103347	-0.096151
12	N	-2.291065	0.064808	-0.031198
13	C	-1.793108	1.384869	-0.030591
14	O	-2.011233	-2.209788	-0.114426
15	O	-2.550923	2.341756	0.011083
16	C	-3.723844	-0.109127	0.027054
17	C	-4.323178	-0.582028	1.195642

18	C	-5.70113	-0.753181	1.25933
19	C	-6.491352	-0.442904	0.147217
20	C	-5.892878	0.033197	-1.023783
21	C	-4.510562	0.195479	-1.081068
22	O	-7.840491	-0.625081	0.264464
23	N	4.194747	-0.414845	-0.093547
24	C	4.74223	0.117632	1.172883
25	C	6.153403	0.672715	0.968658
26	C	7.076713	-0.391684	0.361363
27	C	6.445497	-0.989708	-0.90228
28	C	5.025936	-1.498844	-0.627214
29	H	-0.45908	3.661095	-0.115683
30	H	2.022225	3.993141	-0.308687
31	H	3.524936	2.037087	-0.354785
32	H	2.822273	-2.735282	-0.21422
33	H	0.359296	-2.986409	-0.231509
34	H	-3.705769	-0.821631	2.054757
35	H	-6.180915	-1.123218	2.158729
36	H	-6.504877	0.276904	-1.889311
37	H	-4.043634	0.566138	-1.987153
38	H	-8.266179	-0.373071	-0.5654
39	H	4.072364	0.890171	1.553082
40	H	4.76835	-0.686808	1.930815
41	H	6.10245	1.542888	0.301755
42	H	6.544354	1.023768	1.930651
43	H	8.060852	0.033678	0.135872
44	H	7.240281	-1.190217	1.098589
45	H	6.397862	-0.227575	-1.689666
46	H	7.054425	-1.816476	-1.28563
47	H	4.568162	-1.861133	-1.551828
48	H	5.077269	-2.352492	0.074561

III. Photophysical Studies:

Preparation of the medium: Deionized water was used throughout all experiments. All experiments were carried out in a HEPES buffer (10 mM, pH = 7.4) with 1% DMSO

(maximum). HEPES buffer was prepared by dissolving solid HEPES in deionized water followed by adjustment of pH by 0.5 (N) NaOH solution.

Preparation of solutions of 4o, 4m, 4p, 4o′, 4m′ and 4p′: Stock solutions of **4o**, **4m**, **4p**, **4o′**, **4m′** and **4p′** (2000 μM) were prepared in DMSO. Final concentration of each during assay was 10 μM with 1% DMSO (maximum).

Preparation of the solution of analytes: Stock solutions of NaN_3, KI, Alanine, Lysine, Arginine, Tyrosine, Serine, Glutathione (GSH) and Cysteine (Cys) were prepared in deionized water (concentrations 20 mM). Stock solutions of phenol and Aniline were prepared in DMSO (concentrations 20 mM). Calculated volumes of analytes were added from respective stock solutions to each fluorescence cuvette to provide 100 μM. All spectral data were recorded at 2 min after the addition of analyte(s) by exciting at 425 nm. The excitation and emission slit width were 2 nm and 3 nm, respectively.

Determination of reaction rate (k) and half-life ($t_{1/2}$): Reaction rate (k), half-life ($t_{1/2}$) and response time (t_R) for probe **4o** was determined by fluorescence kinetics experiments. In fluorescence kinetics experiment, PhSH (100 μM) was added to the solution of probe **4o** (10μM) in HEPES buffer (10 mM, pH = 7.4, 1.0% DMSO) placed in a cuvette at room temperature at t = 60 s and fluorescence intensity was recorded at λ = 548 nm (upon λ_{ex} = 425 nm). Rate constant, k and response time (t_R) for probe **4o** was determined according to the following equation (Eq. S1):

$$Y = a \times [1 - e^{(-kt)}] \qquad \textbf{Eq. S1}$$

where, Y = fractional fluorescence intensity, a = arbitrary constant, k = pseudo first order rate constant, t = time.

Half-life of the reaction ($t_{1/2}$) was calculated using Eq. S2

$$t_{1/2} = 0.693/k \qquad \textbf{Eq. S2}$$

where k = pseudo first order rate constant.

Determination of quantum yields: The quantum yield was determined according to the Eq. S3:

$$\Phi = \Phi_S \times [(I \times A_S \times \lambda_{ex(S)} \times \eta^2)/[(I_S \times A \times \lambda_{ex} \times \eta_S^2)] \qquad \textbf{Eq. S3}$$

where, Φ is quantum yield; I is integrated area under the corrected emission spectra; A is absorbance at the excitation wavelength; λ_{ex} is the excitation wavelength (here, $\lambda_{ex(S)} = \lambda_{ex}$); η is the refractive index of the solution; the subscript S refers to the standard.

Determination of selectivity: determined according to the following equation Eq. S4:

Relative fluorescence Intensity $= I_F/I_0$ **Eq. S4**

where, I_0 = fluorescence intensity of free probe at 548 nm (λ_{ex} = 425 nm) and I_F = fluorescence intensity at 548 nm (λ_{ex} = 425 nm) after addition of thiophenol to **4o**.

Detection Limit Calculation: Limit of Detection for thiophenol was calculated using fluorometric titrations using equation S5,

$LOD = 3\sigma/m$ **Eq. S5**

where σ = standard deviation of 6 blank measurements and m = slope obtained from the graph of fluorescence intensity *vs.* concentration of thiophenol added.

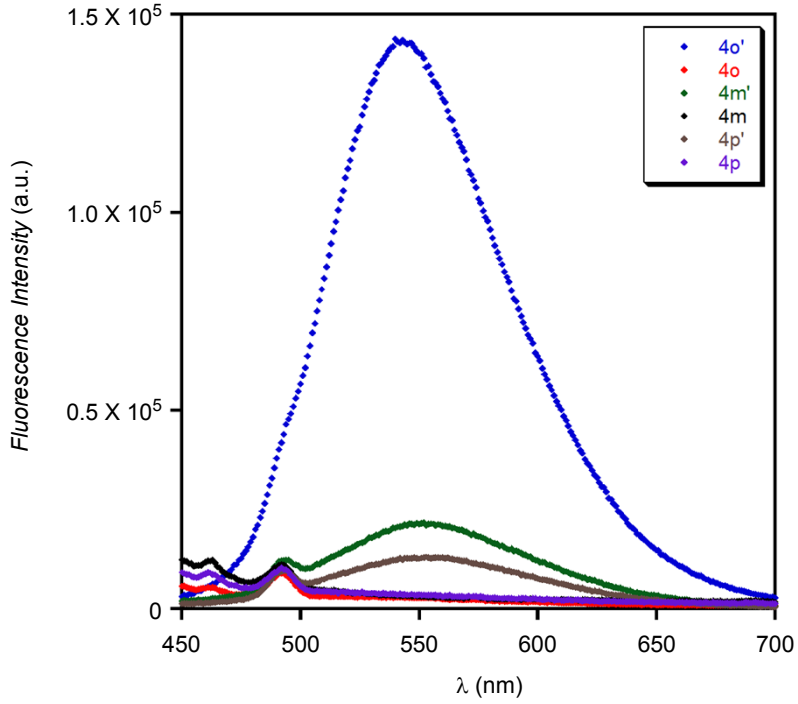

Fig. S4 Fluorescence spectra of compounds **4o**, **4o′**, **4m**, **4m′**, **4p** and **4p′** in HEPES buffer (10 mM, pH 7.4, 1% DMSO). Each sample was of concentration = 10 μM and spectrum was recorded with λ_{ex} = 425 nm.

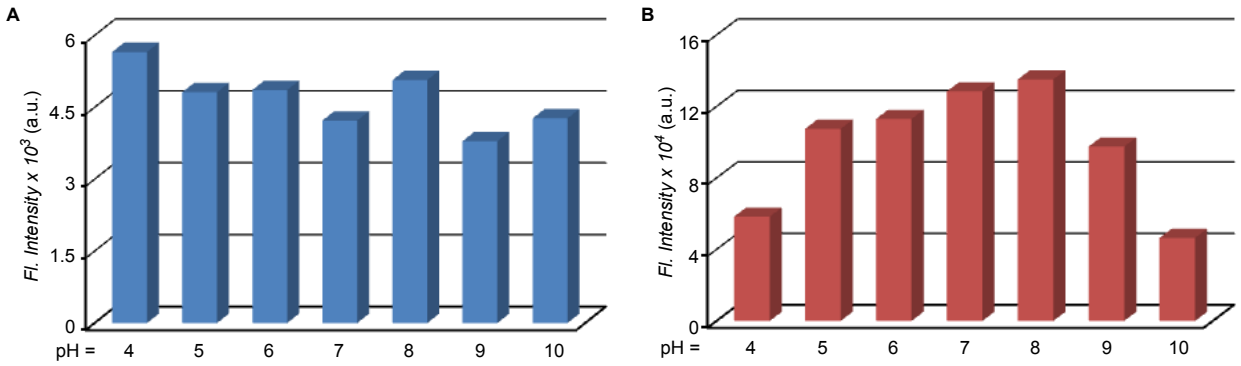

Fig. S5 Fluorescence intensity of probe **4o** (10 μM) before (**A**) and after (**B**) addition of 100 μM PhSH in HEPES buffer (10 mM) of different pH. Each spectrum was recorded after 6 min of PhSH addition (λ_{ex} = 425 nm). Bar plot was generated by recording intensity at 548 nm.

IV. Mass (ESI-MS) analysis of reaction mixture of probe 4o with PhSH:

The samples were prepared in acetonitrile by mixing of **4o** and PhSH in equimolar quantity (100 μM each after mixing). The sample was electrosprayed as 20 μM solutions of **4o** and PhSH in acetonitrile at flow rates of 0.4 mL/min. A constant spray and highest intensities were achieved with a capillary voltage of 3000 V at a source temperature of 80 °C. The parameters for sample cone (45 V) and extractor cone voltage (5 V) were optimized for maximum intensities of the desired complexes. Fig. S6 represents the ESI-MS data recorded showed the presence of **4o′** from acetonitrile solution of **4o** and PhSH . From the spectrum, signals corresponding to [**4o′**+H]$^+$, [**4o′**+Na]$^+$, [**4o**+H]$^+$, [**4o**+Na]$^+$ and [**4o′**+K]$^+$ were observed.

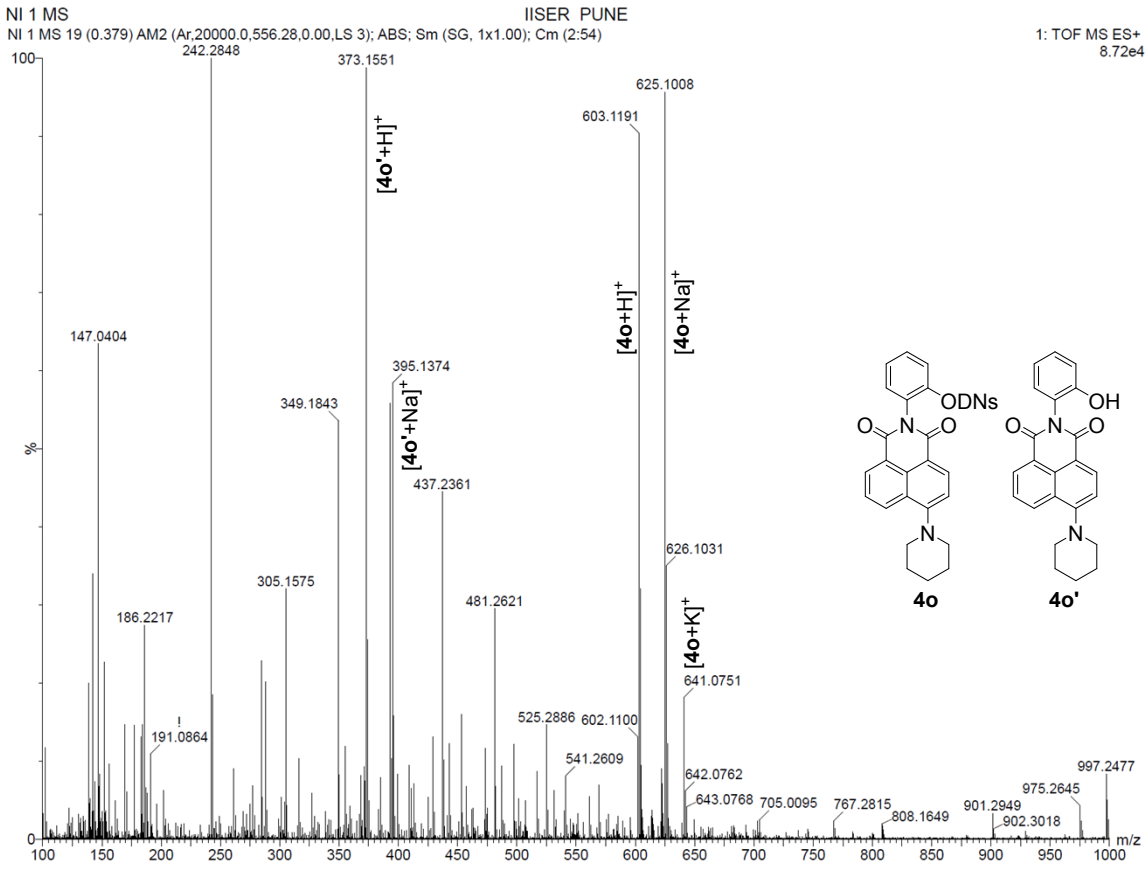

Fig. S6 ESI-MS spectrum of the probe **4o** titrated with PhSH in acetonitrile.

VII. NMR Spectra:

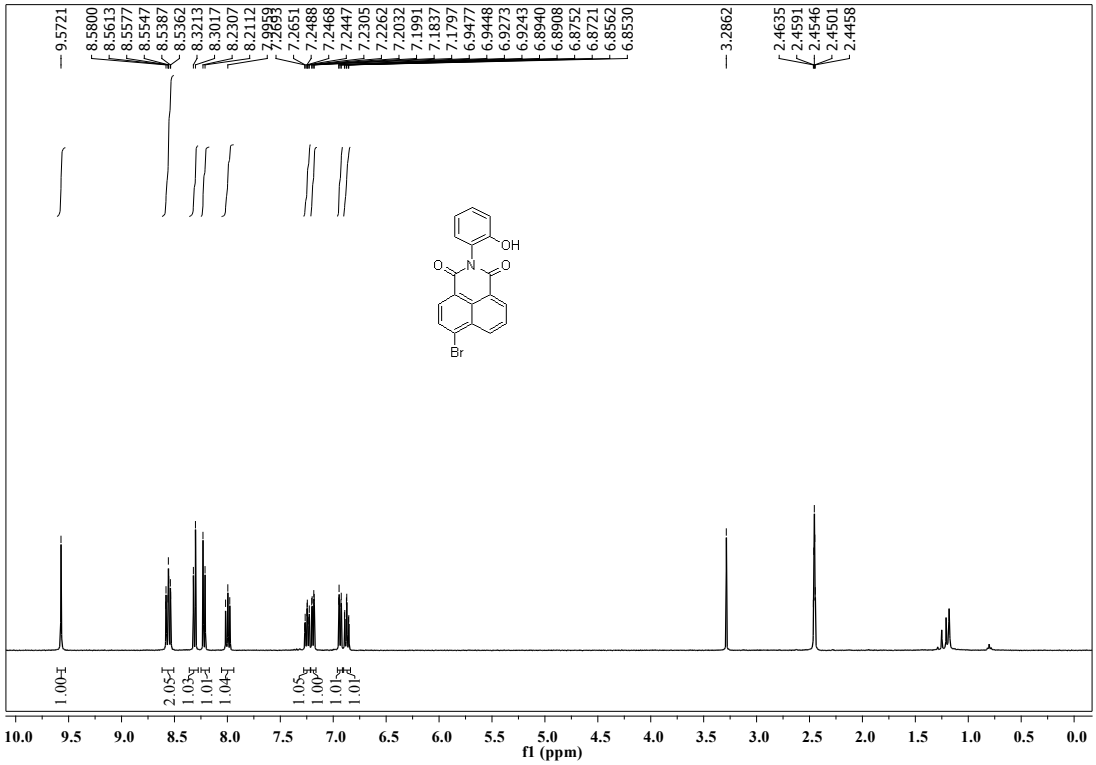

Fig. S7 ^{1}H NMR spectrum of **7a** in DMSO-D_6.

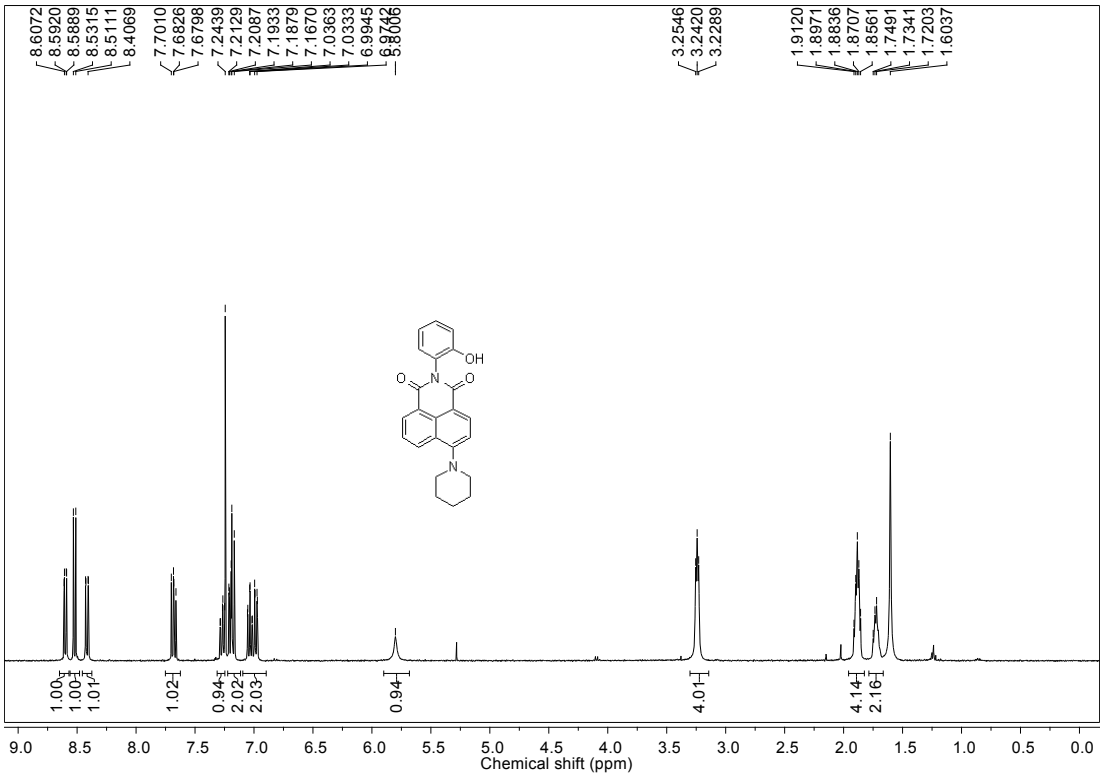

Fig. S8 ^{1}H NMR spectrum of **4o′** in $CDCl_3$.

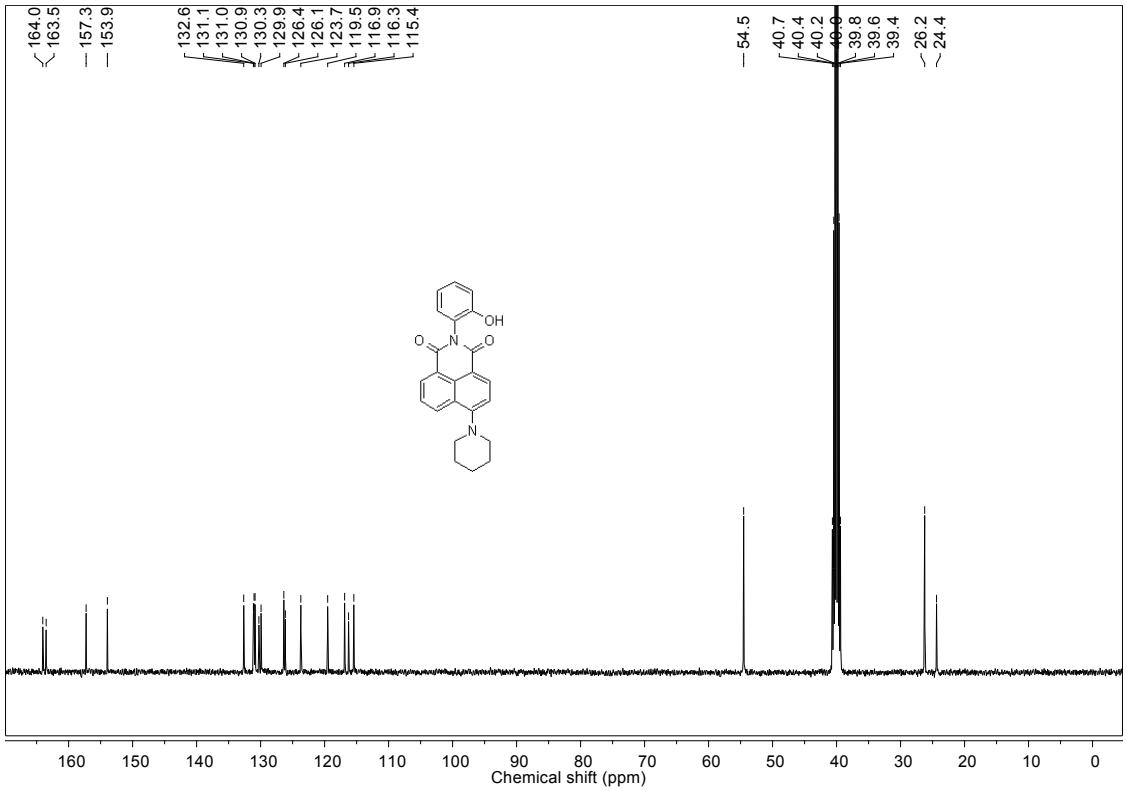

Fig. S9 ^{13}C NMR spectrum of **4o′** in DMSO-D_6.

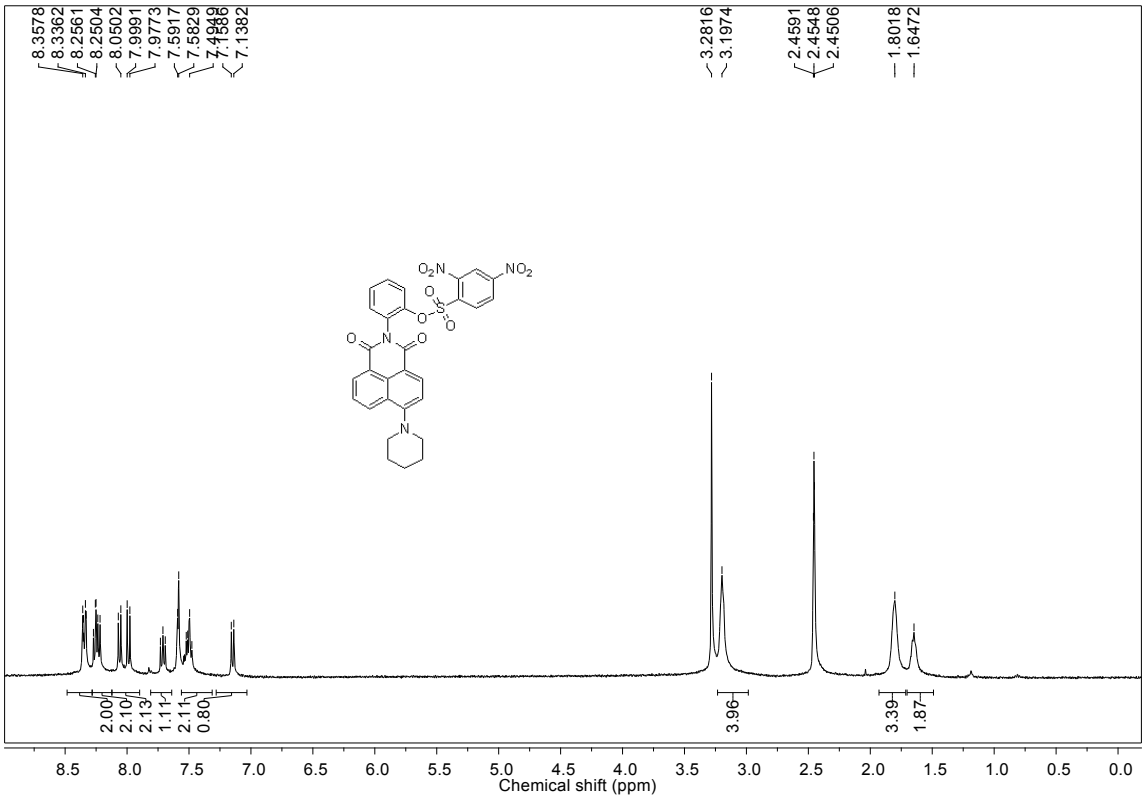

Fig. S10 ^{1}H NMR spectrum of **4o** in DMSO-D_6.

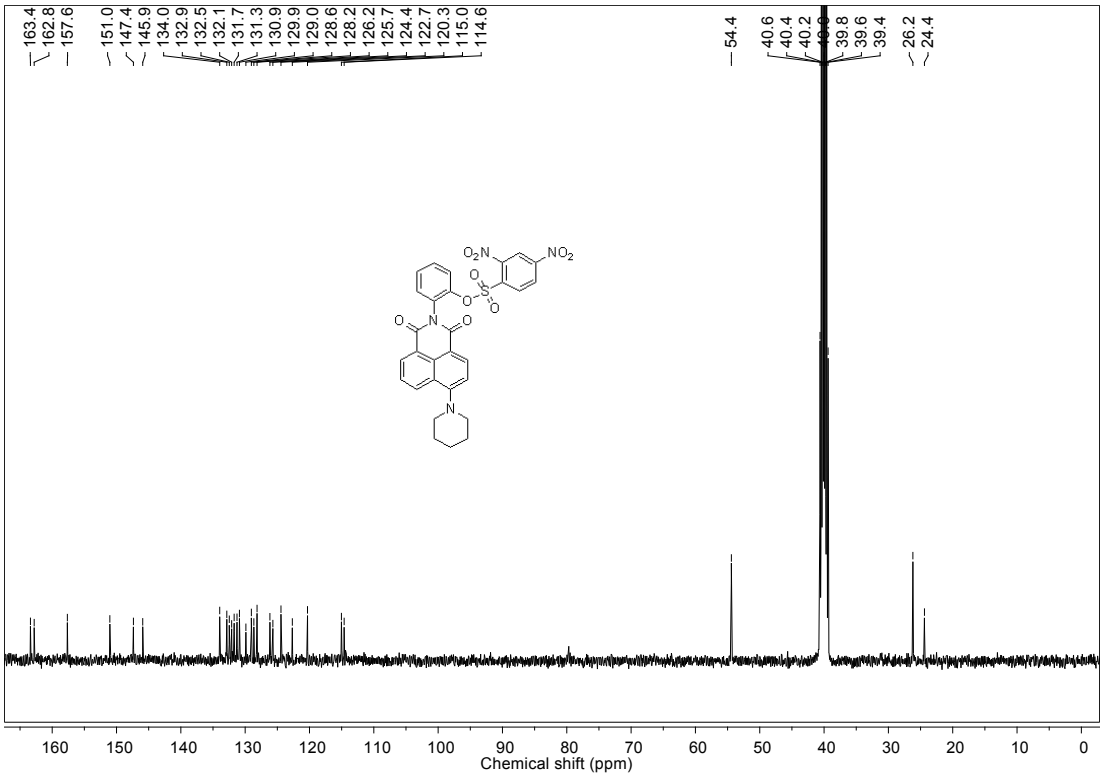

Fig. S11 ^{13}C NMR spectrum of **4o** in DMSO-D_6.

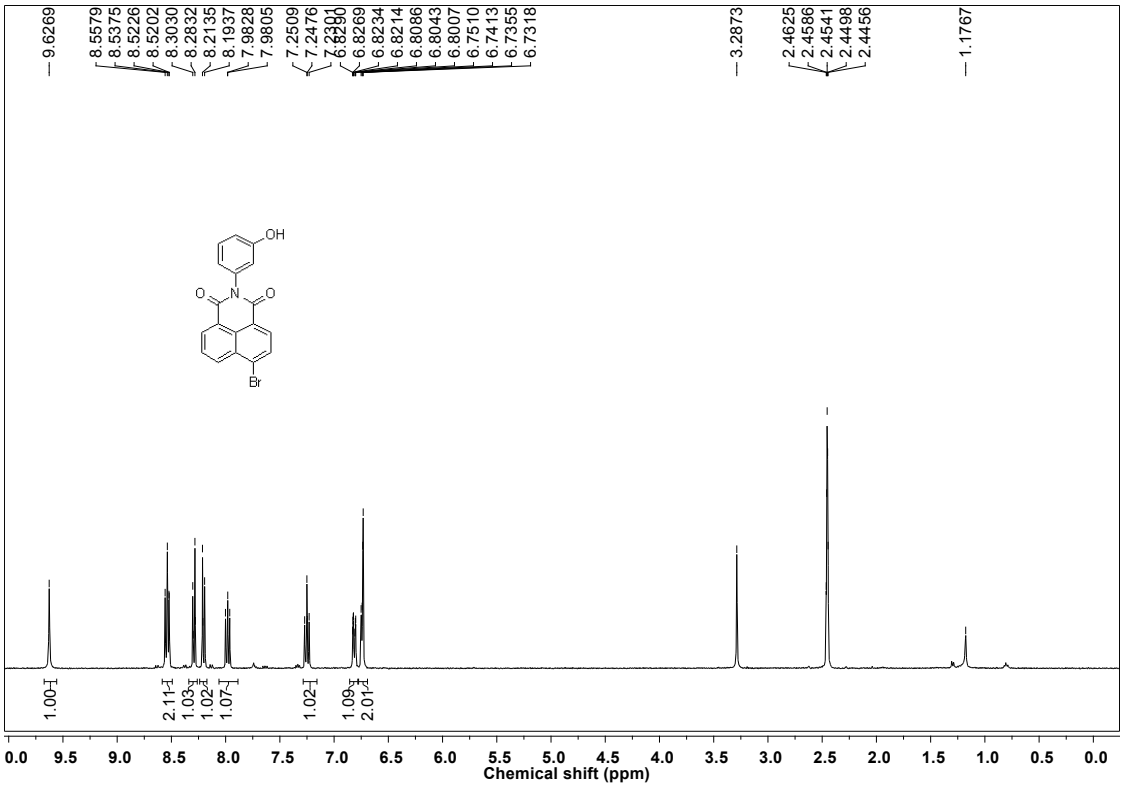

Fig. S12 ^{1}H NMR spectrum of **7b** in DMSO-D_6.

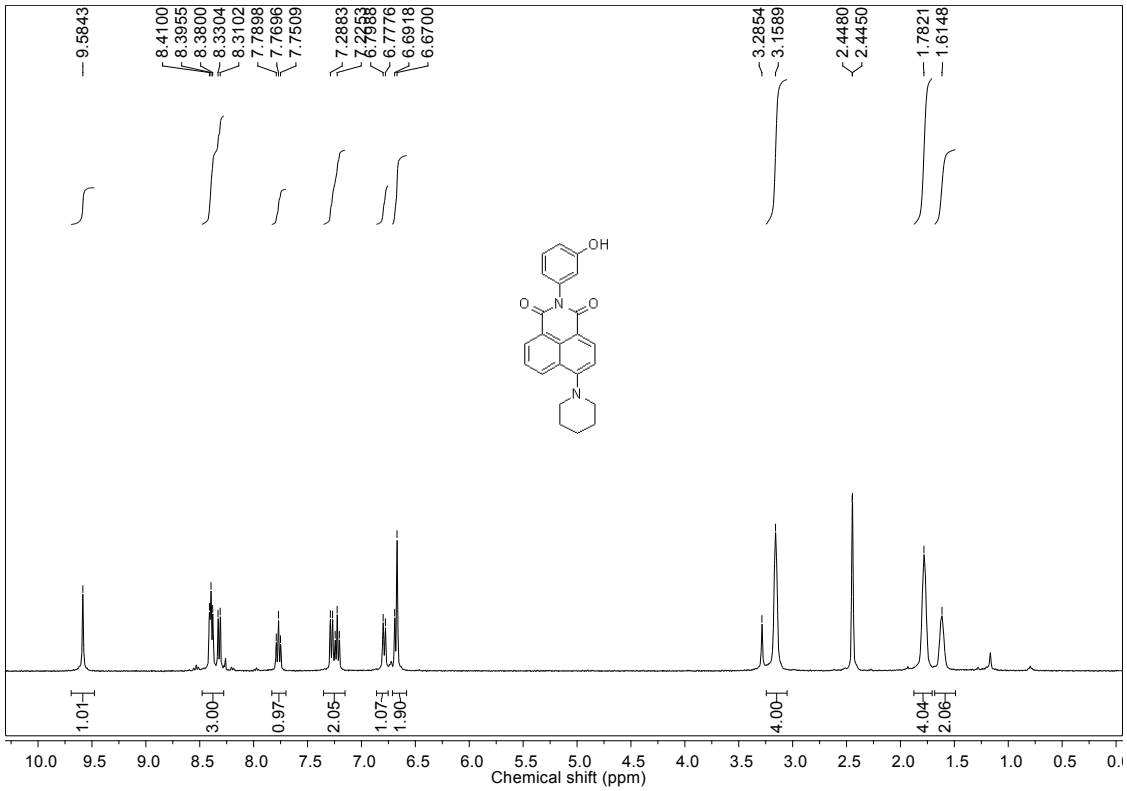

Fig. S13 ^{1}H NMR spectrum of **4m′** in DMSO-D_6.

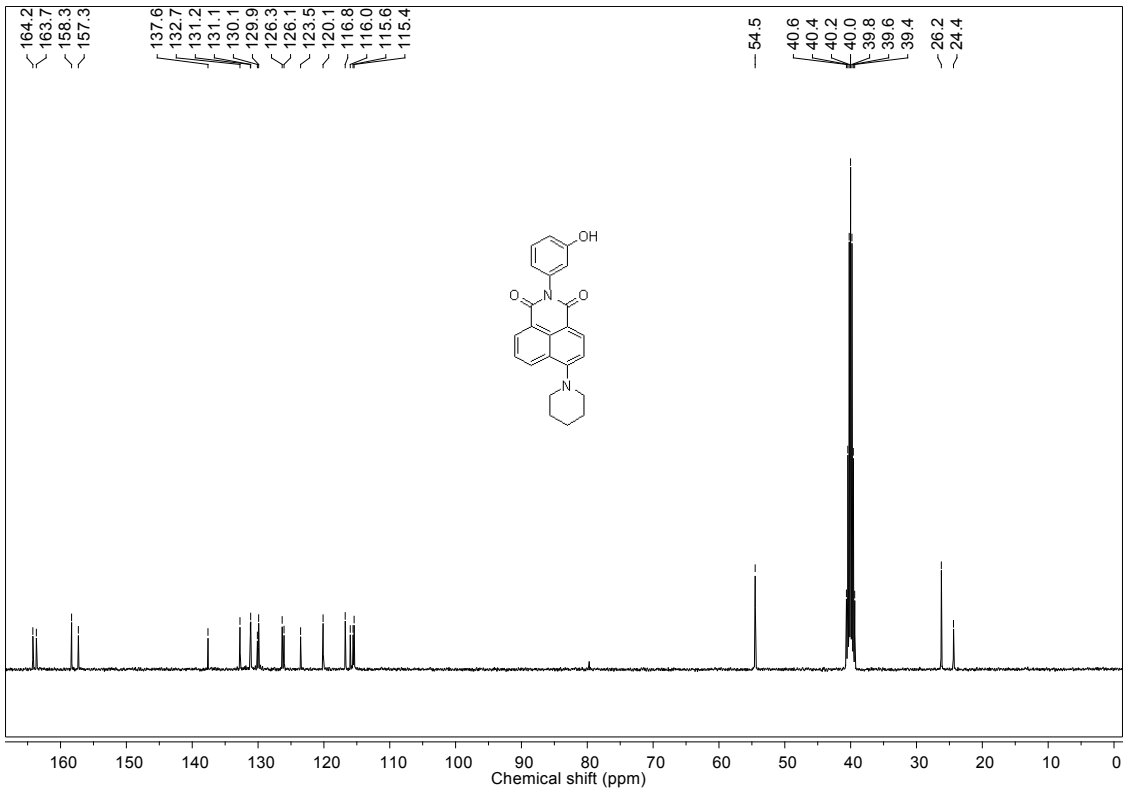

Fig. S14 ^{13}C NMR spectrum of **4m′** in DMSO-D_6.

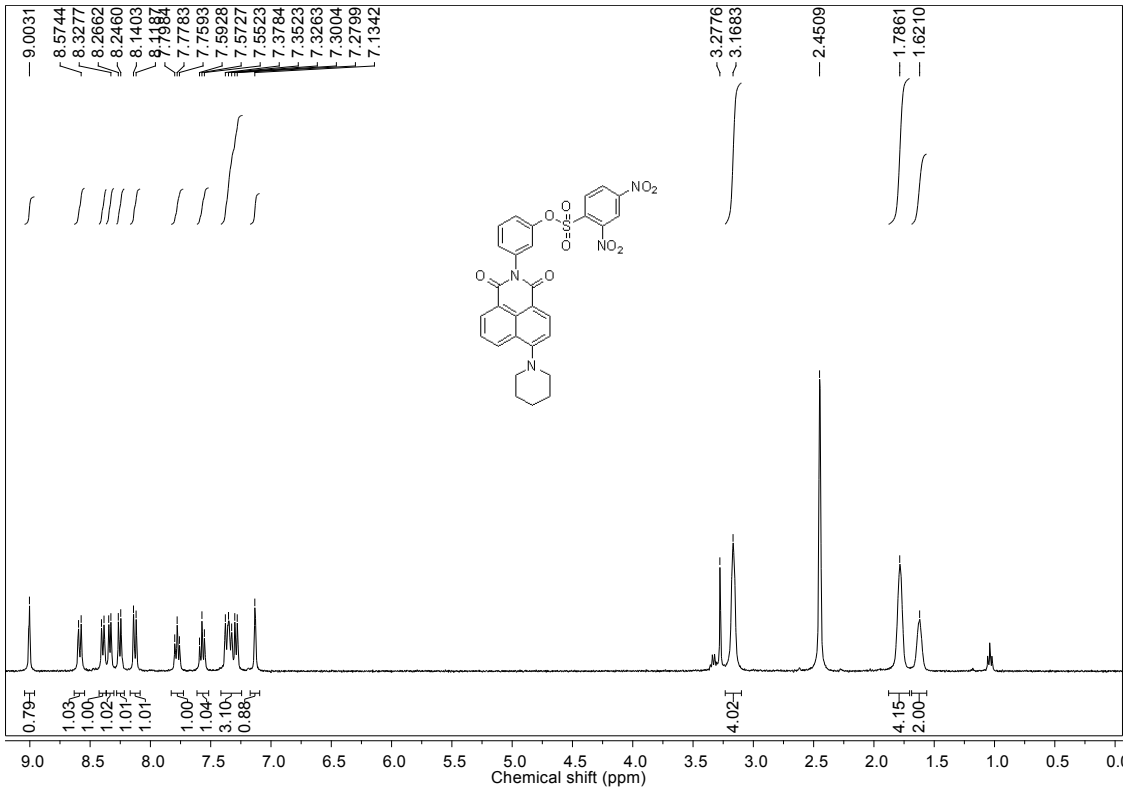

Fig. S15 ^{1}H NMR spectrum of **4m** in DMSO-D_6.

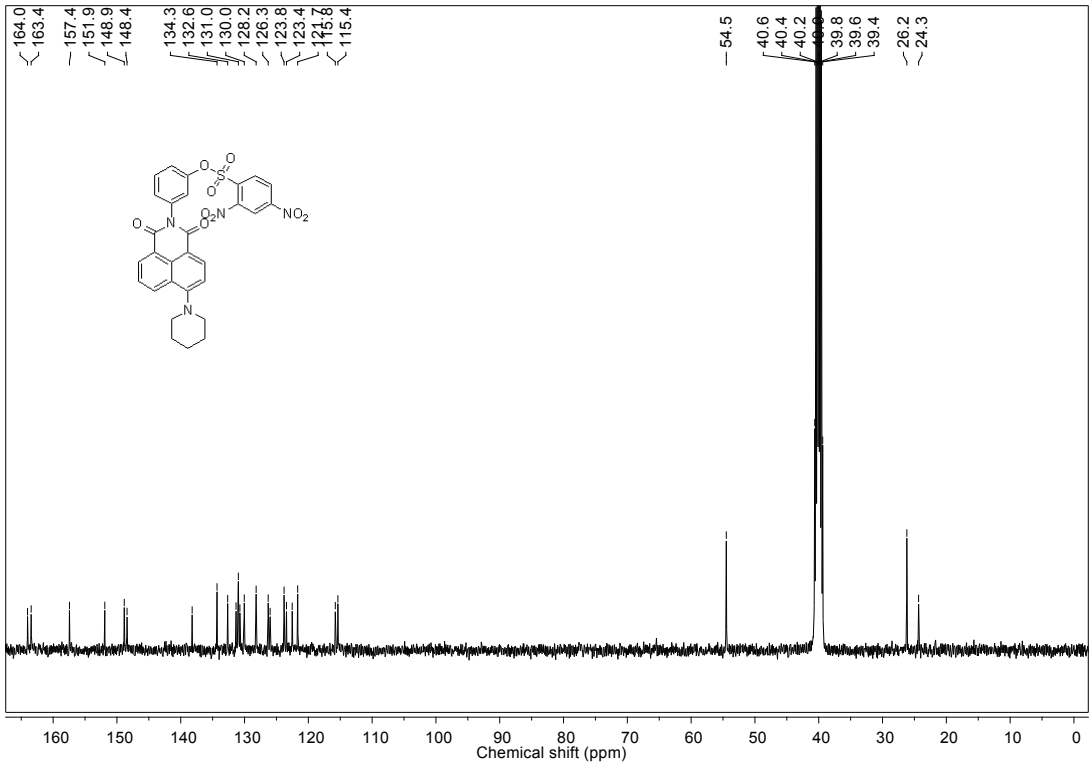

Fig. S16 ^{13}C NMR spectrum of **4m** in DMSO-D_6.

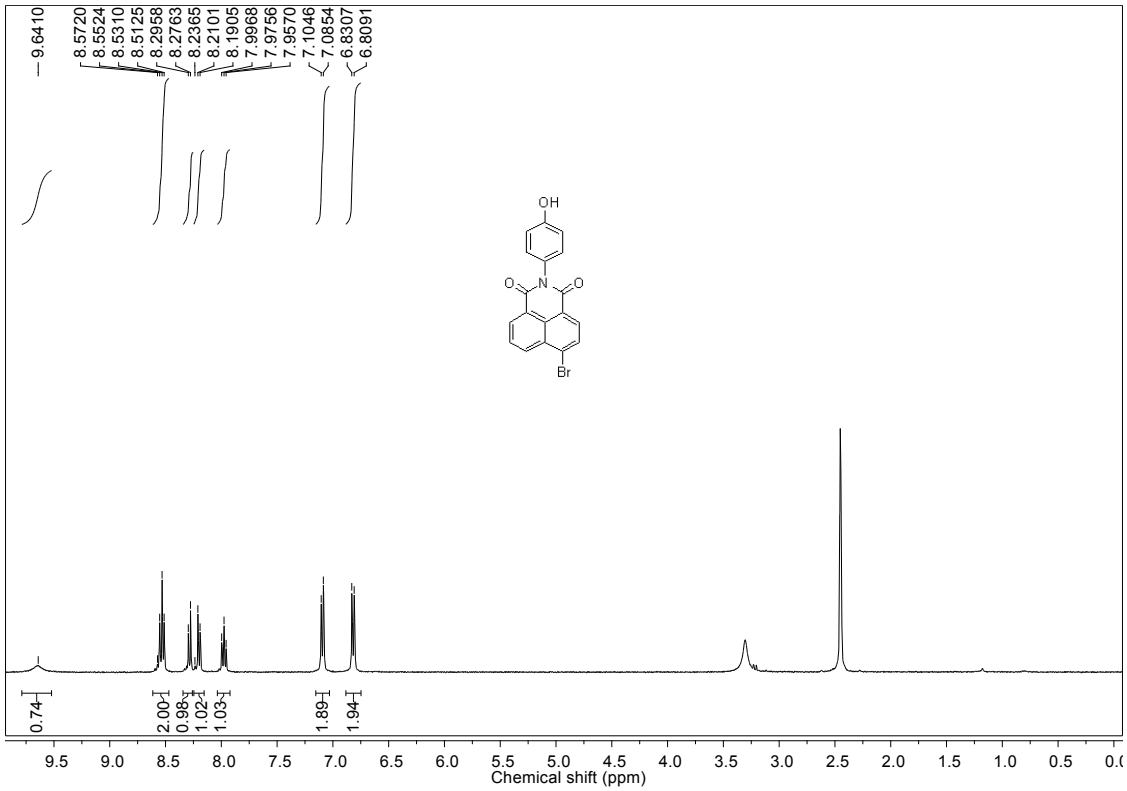

Fig. S17 ^{1}H NMR spectrum of **7c** in DMSO-D_6.

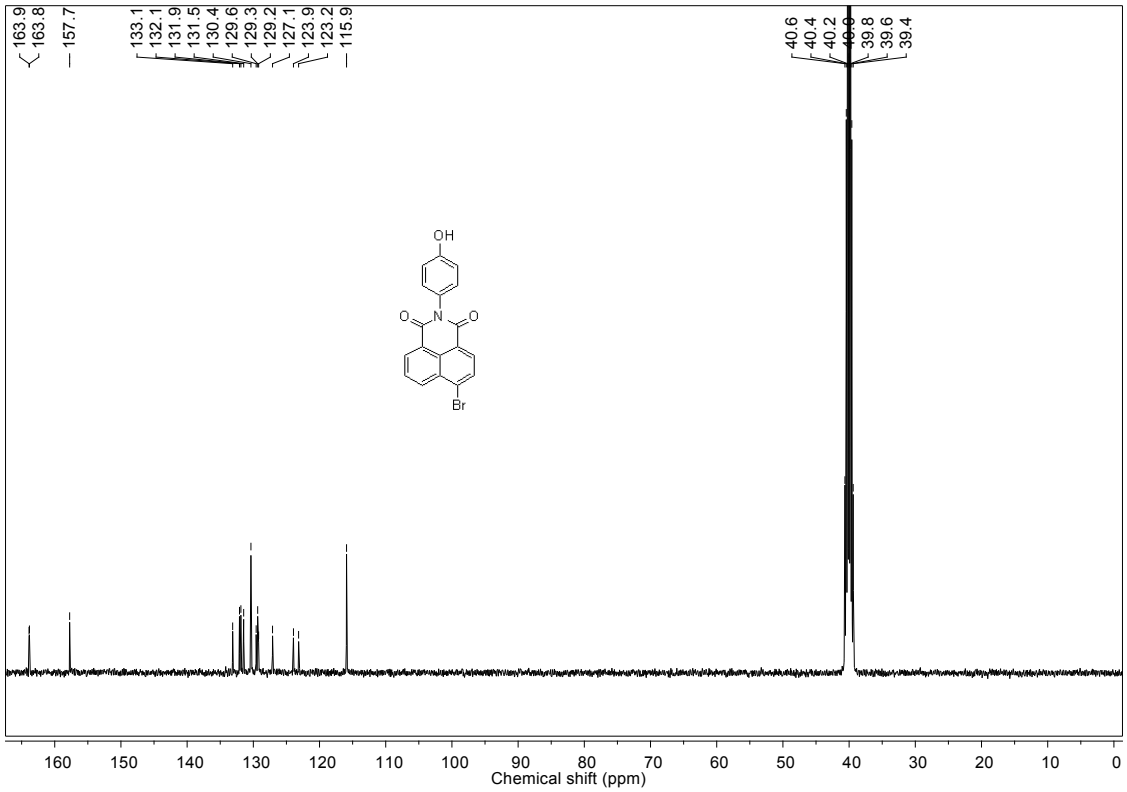

Fig. S18 ^{13}C NMR spectrum of **7c** in DMSO-D_6.

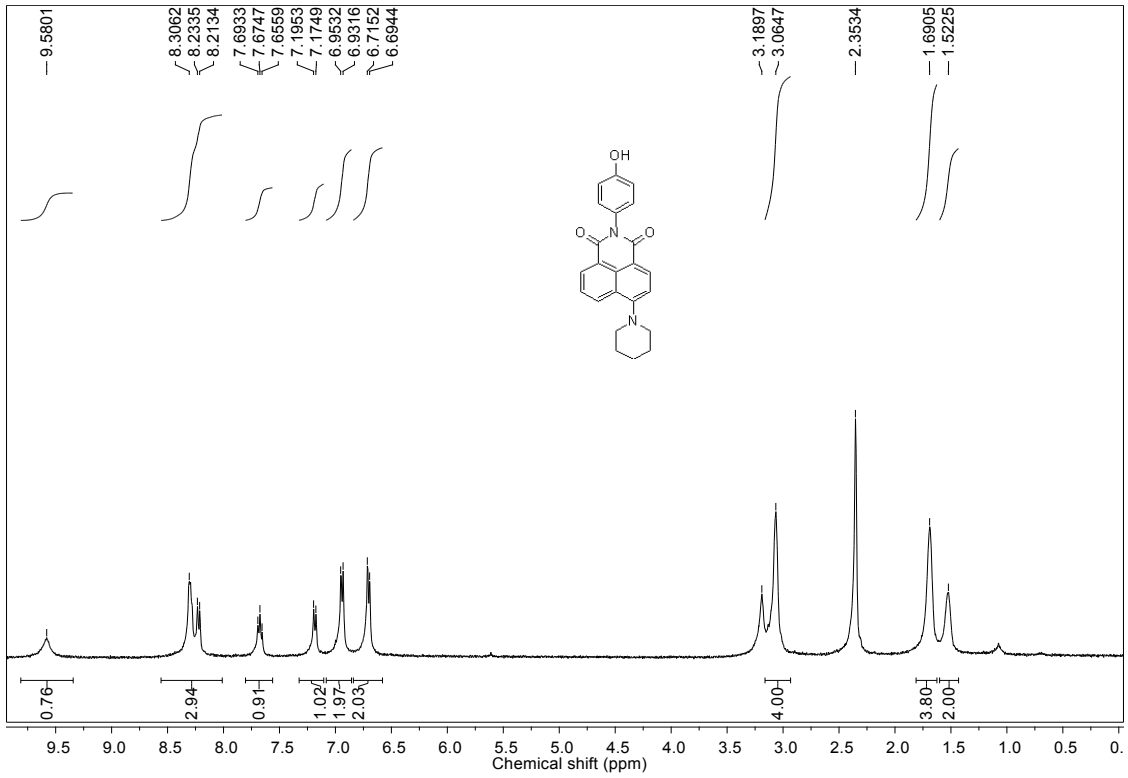

Fig. S19 ^{1}H NMR spectrum of **4p′** in DMSO-D_6.

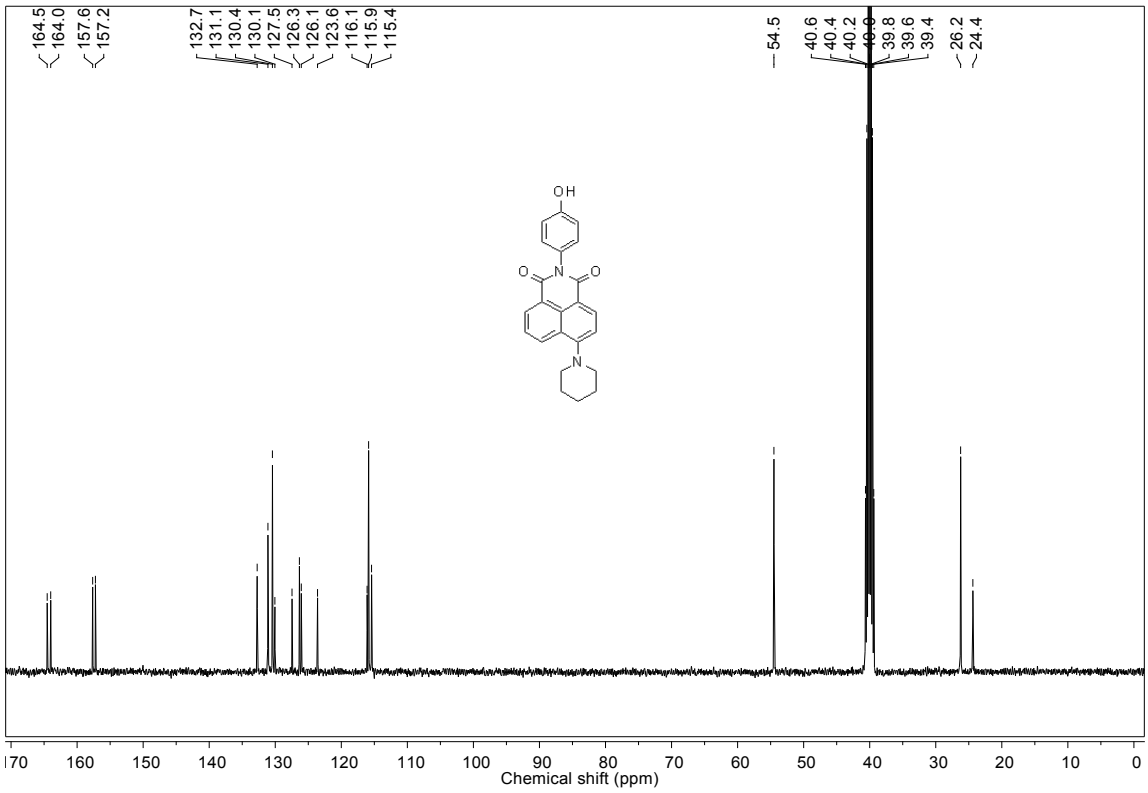

Fig. S20 ^{13}C NMR spectrum of **4p′** in DMSO-D_6.

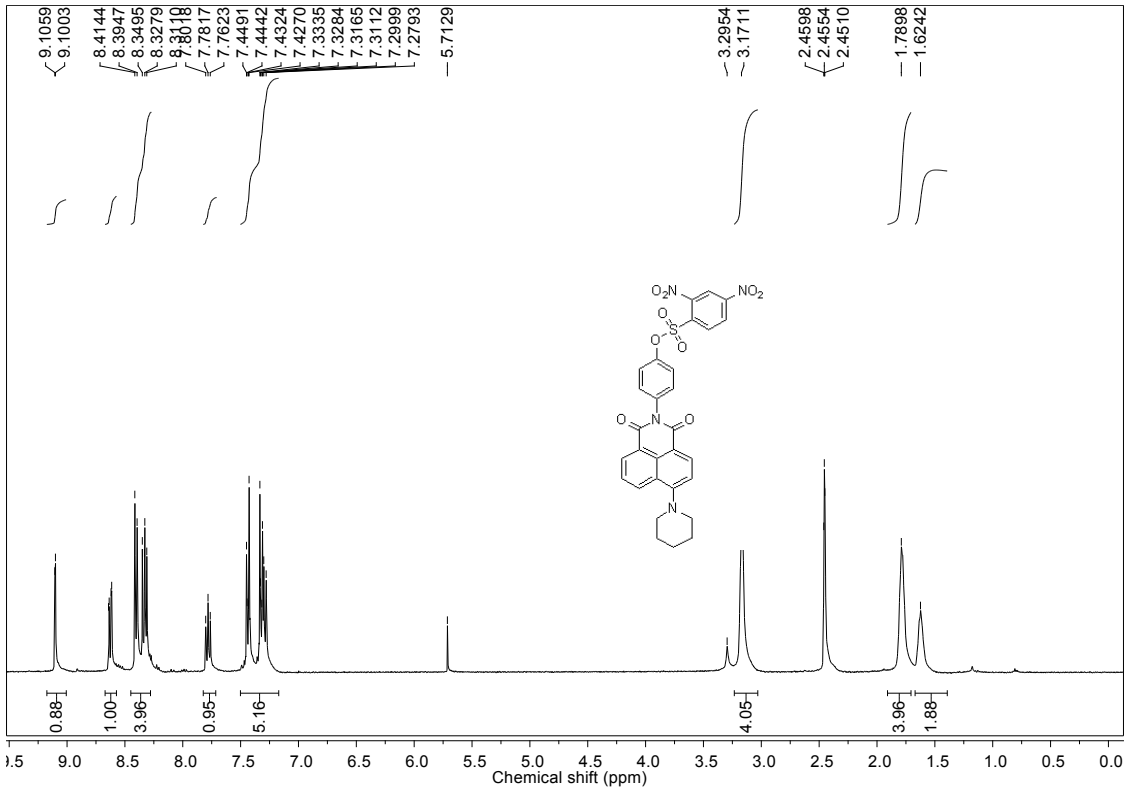

Fig. S21 ^{1}H NMR spectrum of **4p** in DMSO-D_6.

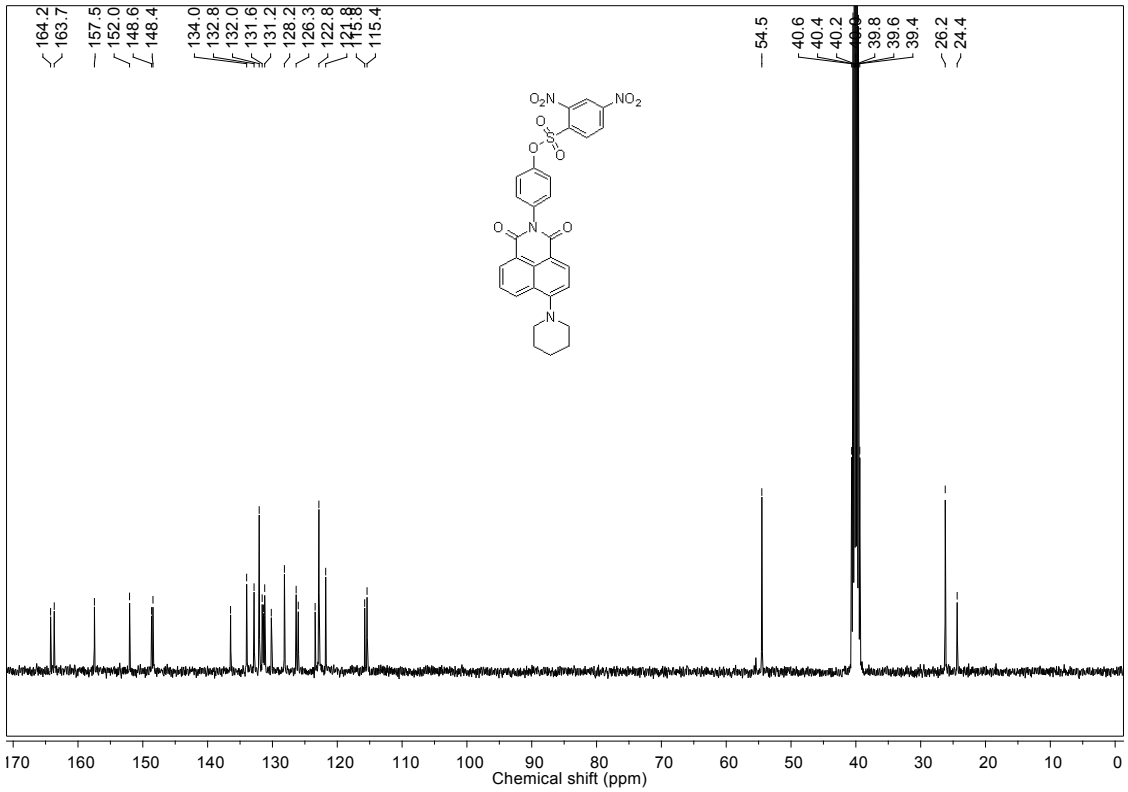

Fig. S22 ^{13}C NMR spectrum of **4p** in DMSO-D_6.

VI. References.

S1. Frisch, M. J.; Trucks, G. W.; Schlegel, H. B.; Scuseria, G. E.; Robb, M. A.; Cheeseman, J. R.; Scalmani, G.; Barone, V.; Mennucci, B.; Petersson, G. A.; Nakatsuji, H.; Caricato, M.; Li, X.; Hratchian, H. P.; Izmaylov, A. F.; Bloino, J.; Zheng, G.; Sonnenberg, J. L.; Hada, M.; Ehara, M.; Toyota, K.; Fukuda, R.; Hasegawa, J.; Ishida, M.; Nakajima, T.; Honda, Y.; Kitao, O.; Nakai, H.; Vreven, T.; Montgomery, Jr. J. A.; Peralta, J. E.; Ogliaro, F.; Bearpark, M.; Heyd, J. J.; Brothers, E.; Kudin, K. N.; Staroverov, V. N.; Kobayashi, R.; Normand, J.; Raghavachari, K.; Rendell, A.; Burant, J. C.; Iyengar, S. S.; Tomasi, J.; Cossi, M.; Rega, N.; Millam, J. M.; Klen, M.; Knox, J. E.; Cross, J. B.; Bakken, V.; Adamo, C.; Jaramillo, J.; Gomperts, R.; Stratmann, R. E.; Yazyev, O.; Austin, A. J.; Camm, R.; Pomelli, C.; Ochterski, J. W.; Martin, R. L.; Morokuma, K.; Zakrzewski, V. G.; Voth, G. A.; Salvador, P.; Dannenberg, J. J.; Dapprich, S.; Daniels, A. D.; Farkas, Ö.; Foresman, J. B.; Ortiz, J. V.; Cioslowski, J.; Fox, D. J. Gaussian, Inc., Wallingford CT, **2009**.